Gain-of-function/Noonan syndrome SHP-2/*Ptpn11* mutants enhance calcium oscillations and impair NFAT signaling

Per Uhlén*, Peter M. Burch, Christina Ivins Zito, Manuel Estrada, Barbara E. Ehrlich, and Anton M. Bennett

Department of Pharmacology, Yale University School of Medicine, New Haven, CT 06520

Communicated by Andrew R. Marks, Columbia University, New York, NY, December 16, 2005 (received for review November 2, 2005)

Gain-of-function mutations in SHP-2/*PTPN11* cause Noonan syndrome, a human developmental disorder. Noonan syndrome is characterized by proportionate short stature, facial dysmorphia, increased risk of leukemia, and congenital heart defects in ≈50% of cases. Congenital heart abnormalities are common in Noonan syndrome, but the signaling pathway(s) linking gain-of-function SHP-2 mutants to heart disease is unclear. Diverse cell types coordinate cardiac morphogenesis, which is regulated by calcium (Ca^{2+}) and the nuclear factor of activated T-cells (NFAT). It has been shown that the frequency of Ca^{2+} oscillations regulates NFAT activity. Here, we show that in fibroblasts, Ca^{2+} oscillations in response to FGF-2 require the phosphatase activity of SHP-2. Conversely, gain-of-function mutants of SHP-2 enhanced FGF-2-mediated Ca^{2+} oscillations in fibroblasts and spontaneous Ca^{2+} oscillations in cardiomyocytes. The enhanced frequency of cardiomyocyte Ca^{2+} oscillations induced by a gain-of-function SHP-2 mutant correlated with reduced nuclear translocation and transcriptional activity of NFAT. These data imply that gain-of-function SHP-2 mutants disrupt the Ca^{2+} oscillatory control of NFAT, suggesting a potential mechanism for congenital heart defects in Noonan syndrome.

calcium signaling | cardiomyocytes | FGF | receptor tyrosine kinase signaling | tyrosine phosphatases

The ubiquitously expressed src homology 2 (SH2)-containing protein tyrosine phosphatase (PTP), SHP-2 (*PTPN11*), regulates numerous intracellular signaling cascades that control cell proliferation, differentiation, cell survival, migration, adhesion, and apoptosis (1). SHP-2 contains two NH_2 terminus SH2 domains, a PTP domain, and a COOH terminus containing two tyrosyl phosphorylation sites (1). It is now well established that SHP-2 is required for activation of the extracellular-regulated kinases (ERKs) 1 and 2 in response to the activation of receptor tyrosine kinase (RTK) and cytokine receptors (1). The SH2 domains of SHP-2 mediate not only binding to RTKs but also scaffold proteins such as Gab-1, IRS-1, and FRS-2 (1). In virtually all cases, stimulation of SHP-2 catalysis is required for downstream signaling. The SH2 domains of SHP-2 also regulate its activation. Engagement of the NH_2 SH2 domain of SHP-2 with its cognate phosphotyrosyl protein results in its activation. The mechanism of this activation involves displacement of the NH_2 SH2 domain from the PTP domain which in the basal (unbound SH2 domain) state occludes the PTP active site. Upon NH_2 SH2 domain binding, a conformational relief of this inhibitory state is achieved and the phosphatase becomes active. Insights from the crystallographic structure of SHP-2 (2) resulted in the generation of engineered mutations at residues critical for the maintenance of the basal inactivated state of SHP-2. These mutations, within the NH_2 SH2 domain of SHP-2 (e.g., E76A), generated a constitutively active (gain-of-function) form of SHP-2 that is still capable of interacting appropriately with its upstream phosphotyrosyl target (3).

Genetic disruption of SHP-2 expression in mice results in early embryonic lethality (4). During embryogenesis, SHP-2 has been implicated in the formation of cardiac semilunar valvulogenesis and limb development (5, 6). Germ-line missense mutations of human *PTPN11*, which encodes SHP-2, cause Noonan syndrome, a human autosomal dominant disorder that occurs with an incidence between 1 in 1,000 and 1 in 2,500 live births (7–10). Mutations in SHP-2 that are associated with Noonan syndrome result in its constitutive activation (11). Noonan syndrome is a clinically heterogenous disorder defined by facial dysmorphia and proportionate short stature (7, 8). Congenital heart disease is present in up to 85% of Noonan syndrome patients, constituting the most common nonchromosomal cause of congenital heart disease (7). Pulmonic stenosis is a common form of cardiac disease in Noonan syndrome with a lesser frequency of occurrence of atrioventricular, ventricular septal, and hypertrophic cardiomyopathy. A knock-in mouse model of the Noonan syndrome mutant, D61G, exhibits similar cardiac defects in the atrioventricular and outflow-tract valves (12). These observations support a causal role for SHP-2 gain-of-function mutants in cardiac pathogenesis. Cardiac morphogenesis depends on intracellular calcium (Ca^{2+}), which activates the calcineurin/nuclear factor of activated T-cells (NFAT) pathway (13–16). The regulation of calcineurin by Ca^{2+} is complex because calcineurin/NFAT activity is stimulated not merely by an influx of intracellular Ca^{2+}, but also by the oscillatory frequency of intracellular Ca^{2+} transients (17–19). Given the fundamental role of Ca^{2+} in the regulation of gene expression and activity, we tested whether SHP-2 regulates Ca^{2+} signaling, and if so, whether Ca^{2+} is a target of the effects of gain-of-function SHP-2 mutants that are associated with Noonan syndrome.

Results

SHP-2 Is Required for RTK-Induced Ca^{2+} Signaling. We first examined Ca^{2+} signaling in fibroblasts derived from mice containing a deletion within exon 3 of SHP-2 (SHP-$2^{Ex3-/-}$) that results in the truncation of its NH_2 terminus SH2 domain (4). SHP-$2^{Ex3-/-}$ fibroblasts exhibit properties consistent with a loss of SHP-2 function. Both wild-type (WT) (SHP-$2^{+/+}$) and SHP-$2^{Ex3-/-}$ fibroblasts loaded with Fluo-4/AM responded to ATP, a G protein coupled receptor agonist, by increasing their levels of intracellular Ca^{2+} (Fig. 1 *a* and *b* and Table 1). Similar results were obtained when fibroblasts were exposed to another G protein coupled receptor agonist, bradykinin (data not shown). When fibroblasts were stimulated with platelet-derived growth factor (PDGF), a transient increase in Ca^{2+} was observed in SHP-$2^{+/+}$, but not in SHP-$2^{Ex3-/-}$, fibroblasts (Fig. 1 *c* and *d* and Table 1). Exposing SHP-$2^{Ex3-/-}$ fibroblasts to ATP after stimulation with PDGF, however, resulted in a Ca^{2+} transient (Fig. 1*d*). These results

Conflict of interest statement: No conflicts declared.

Abbreviations: NFAT, nuclear factor of activated T cells; $InsP_3R$, inositol 1,4,5-trisphosphate receptor; RTK, receptor tyrosine kinase; PTP, protein tyrosine phosphatase; SH2, src homology 2; PDGF, platelet-derived growth factor; CPA, cyclopiazonic acid; FDHM, full duration at half maxima.

*To whom correspondence should be sent at the present address: Department of Medical Biochemistry and Biophysics, Karolinska Institutet, Sheelesv. 1, A1:02, SE-17177 Stockholm, Sweden. E-mail: per.uhlen@ki.se.

© 2006 by The National Academy of Sciences of the USA

www.pnas.org/cgi/doi/10.1073/pnas.0510876103

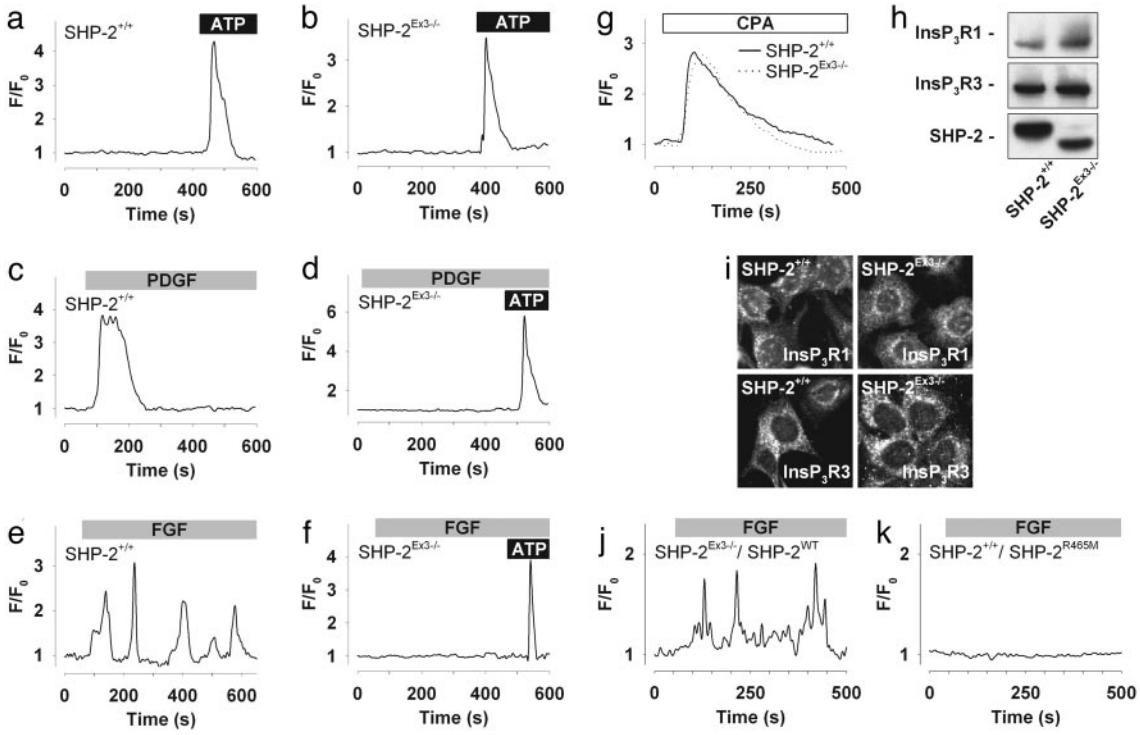

Fig. 1. SHP-2 is required for RTK-generated Ca^{2+} signaling. (*a–g*) Representative single cell Ca^{2+} recordings of Fluo-4/AM-loaded WT (SHP-$2^{+/+}$) (*a*, *c*, *e*, and *g*) and SHP-$2^{Ex3-/-}$ (*b*, *d*, *f*, and *g*) fibroblasts treated with 10 μM ATP (*a* and *b*), 50 ng·ml^{-1} PDGF (*c* and *d*), 100 ng·ml^{-1} FGF-2 (*e* and *f*), and 20 μM CPA (*g*). Ratio F/F_0 represents fluorescence intensity over baseline. (*h*) Immunoblotting of $InsP_3Rs$ type-1 ($InsP_3R1$), type-3 ($InsP_3R3$), and SHP-2 in SHP-$2^{+/+}$ and SHP-$2^{Ex3-/-}$ fibroblasts. (*i*) Immunocytochemistry of $InsP_3R1$ and $InsP_3R3$ in SHP-$2^{+/+}$ and SHP-$2^{Ex3-/-}$ fibroblasts. (*j*) Ca^{2+} recordings in SHP-$2^{Ex3-/-}$ fibroblast transiently transfected with SHP-2^{WT} (SHP-$2^{Ex3-/-}$/SHP-2^{WT}) exposed to 100 ng·ml^{-1} FGF-2. (*k*) Ca^{2+} recordings in WT (SHP-$2^{+/+}$) fibroblast expressing catalytically inactive SHP-2^{R465M} (SHP-$2^{+/+}$/SHP-2^{R465M}) exposed to 100 ng·ml^{-1} FGF-2.

demonstrate that SHP-2 is required for PDGF-induced, but not ATP-induced, increases in intracellular Ca^{2+}. To further investigate the generality of SHP-2 to regulate intracellular Ca^{2+} signaling by RTKs, SHP-$2^{+/+}$ and SHP-$2^{Ex3-/-}$ fibroblasts were exposed to fibroblast growth factor-2 (FGF-2). Unlike PDGF, which caused a Ca^{2+} transient, FGF-2 evoked Ca^{2+} oscillations in SHP-$2^{+/+}$ fibroblasts (Fig. 1*e* and Table 1), whereas SHP-$2^{Ex3-/-}$ fibroblasts were unresponsive to FGF-2 stimulation (Fig. 1*f* and Table 1). We found that FGF-2 (100 ng·ml^{-1}) failed to elicit Ca^{2+} oscillations in SHP-$2^{Ex3-/-}$ fibroblasts, but ≈50% of SHP-$2^{+/+}$ fibroblasts evoked Ca^{2+} oscillations (Table 1). Hence, SHP-2 is required for the propagation of FGF-2-induced Ca^{2+} oscillations in fibroblasts.

Intact Intracellular Ca^{2+} Stores and Rescue of Ca^{2+} Signaling in SHP-$2^{Ex3-/-}$ Fibroblasts. A pharmacological approach was applied to determine whether the defect in PDGF- and FGF-induced Ca^{2+} responses in SHP-$2^{Ex3-/-}$ fibroblasts was due to intracellular defects in Ca^{2+} stores. First, fibroblasts were treated with cyclopiazonic acid (CPA), a sarcoendoplasmic reticulum Ca^{2+}-ATPase (SERCA) inhibitor, which can be used to deplete intracellular Ca^{2+} stores. Both SHP-$2^{+/+}$ and SHP-$2^{Ex3-/-}$ fibroblasts showed similar Ca^{2+} responses to CPA (Fig. 1*g*), indicating that internal endoplasmic reticulum Ca^{2+} stores were equally intact. Thapsigargin, also a SERCA inhibitor, gave comparable responses (see Fig. 5 *a* and *b*, which is published as supporting information on the PNAS web site). Neither FGF-2 nor PDGF evoked Ca^{2+} responses in SHP-$2^{+/+}$ fibroblasts after internal Ca^{2+} stores were depleted after CPA stimulation (Fig. 5*c*). Mobilization of intracellular Ca^{2+} is mediated by the inositol 1,4,5-trisphosphate receptor ($InsP_3R$) (20). Preincubation of fibroblasts with the $InsP_3R$ inhibitor, 2-aminoethoxydiphenyl borate (2-APB) blocked FGF-2- and PDGF-induced Ca^{2+} responses (Fig. 5*d*). Thus, PDGF and FGF-2 regulate $InsP_3R$-

Table 1. Characteristics of Ca^{2+} responses in WT (SHP-$2^{+/+}$) and SHP-$2^{Ex3-/-}$ fibroblasts exposed to vehicle, ATP (10 μM), PDGF (50 ng·ml^{-1}), or FGF (100 ng·ml^{-1}).

	SHP-$2^{+/+}$				SHP-$2^{Ex3-/-}$			
Treatment	Nonresponding*, %	Transient†, %	Oscillation‡, %	[*n*/*N*]§	Nonresponding*, %	Transient†, %	Oscillation‡, %	[*n*/*N*]§
Vehicle	93 (153)	5 (8)	2 (4)	[165/4]	96 (152)	2 (4)	2 (3)	[159/2]
ATP	53 (86)	46 (73)	1 (3)	[162/3]	47 (63)	52 (69)	1 (1)	[133/3]
PDGF	22 (81)	76 (285)	2 (7)	[373/6]	96 (192)	3 (6)	1 (3)	[201/5]
FGF	32 (49)	18 (28)	50 (78)	[155/4]	89 (155)	9 (16)	2 (4)	[175/6]

*Nonresponding cells have no Ca^{2+} increase exceeding 1.25 of the baseline. Values in parentheses are number of cells.
†Transient responding cells have one Ca^{2+} peak exceeding 1.25 of the baseline. Values in parentheses are number of cells.
‡Oscillatory responding cells have at least three Ca^{2+} peaks exceeding 1.25 of the baseline. Values in parentheses are number of cells.
§[Number of cells/number of experiments].

Table 2. Description of SHP-2 mutants used in this study

SHP-2 mutations	Mutation domain/functional description	Reported disease association
SHP-2^{R465M}-Arg-465 → Met-465	Catalytically inactive/nonsubstrate trapping	—
SHP-2^{E76A}-Glu-76 → Ala-76	NH_2–SH2 domain mutation/enhanced phosphatase activity	Gain-of-function
SHP-2^{D61G}-Asp-61 → Gly-61	NH_2–SH2 domain mutation/enhanced phosphatase activity	Noonan syndrome (ref. 10)

mediated Ca^{2+} increases by controlling the release of internal Ca^{2+} stores. We also investigated whether SHP-$2^{+/+}$ and SHP-$2^{Ex3-/-}$ fibroblasts exhibited differences in Ca^{2+} response as a consequence of altered $InsP_3R$ levels and/or subcellular distribution. SHP-$2^{+/+}$ and SHP-$2^{Ex3-/-}$ fibroblasts showed similar levels of expression of the type 1 and 3 $InsP_3Rs$ (Fig. 1*h*); the type 2 $InsP_3R$, however, was undetectable. Similar subcellular distribution in SHP-$2^{+/+}$ and SHP-$2^{Ex3-/-}$ fibroblasts were observed for both type 1 and 3 $InsP_3Rs$ (Fig. 1*i*). To determine whether SHP-$2^{Ex3-/-}$ fibroblasts express the FGF receptor to levels equivalent to that of SHP-$2^{+/+}$ fibroblasts, we used purified GFP-tagged FGF protein (FGF-GFP) to label these cells. When FGF-GFP was exposed to these fibroblasts, similar levels of plasma membrane FGF-GFP fluorescence was observed in SHP-$2^{+/+}$ and SHP-$2^{Ex3-/-}$ fibroblasts (see Fig. 6 *a* and *b*, which is published as supporting information on the PNAS web site). Together, these results support the interpretation that the impaired Ca^{2+} signaling in SHP-$2^{Ex3-/-}$ fibroblasts is due to a loss of SHP-2 function rather than defects in the Ca^{2+}-generating machinery.

To definitively establish that SHP-2 is responsible for FGF-2-induced Ca^{2+} oscillations, SHP-$2^{Ex3-/-}$ fibroblasts were transfected with WT SHP-2 (SHP-2^{WT}) to rescue the Ca^{2+} signaling defect. We found that SHP-2^{WT} expressing SHP-$2^{Ex3-/-}$ fibroblasts (SHP-$2^{Ex3-/-}$/SHP-2^{WT}) regained their ability to evoke Ca^{2+} oscillations in response to FGF-2 (Fig. 1*j*), but vector control transfectants remained nonresponsive (data not shown). The requirement for SHP-2 to generate Ca^{2+} oscillations in response to FGF-2 depended on SHP-2 catalysis because overexpression of a catalytically inactive mutant of SHP-2 (Table 2), SHP-2^{R465M} in SHP-$2^{+/+}$ fibroblasts (SHP-$2^{+/+}$/SHP-2^{R465M}), failed to elicit a Ca^{2+} response to FGF-2 (Fig. 1*k*). These results demonstrate that loss of SHP-2 is causally related to the attenuated Ca^{2+} response and that the catalytic activity of SHP-2 is required to generate FGF-2-induced Ca^{2+} oscillations.

SHP-2 Gain-of-Function and Noonan Syndrome Mutations Enhance Ca^{2+} Oscillatory Frequency. Because the catalytic activity of SHP-2 is required to mediate Ca^{2+} signaling in response to FGF-2 (Fig. 1*k*), we tested the effects of a constitutively active mutant of SHP-2 (Table 2) on FGF-2-induced Ca^{2+} oscillations. A mutation within the NH_2 terminus SH2 domain of SHP-2 at Glu-76 to Ala-76 (SHP-2^{E76A}) has been shown to result in constitutive SHP-2 catalysis (3). As compared with vector and SHP-2^{WT} expressing fibroblasts, SHP-2^{E76A} expressing fibroblasts exhibited an enhanced oscillatory frequency in response to FGF-2 (Fig. 2 *a–c*; see also Movie 1, which is published as supporting information on the PNAS web site). To quantitate the oscillatory behavior of this response, we performed a spectral analysis (21) of FGF-2-induced Ca^{2+} oscillations in fibroblasts transfected with vector, SHP-2^{WT} and SHP-2^{E76A}. This quantitative analysis revealed that vector control and SHP-2^{WT} expressing fibroblasts exhibited FGF-2-induced Ca^{2+} oscillations with a frequency of 9.6 ± 1.4 mHz (n = 25) and 12.6 ± 1.0 mHz (n = 25), respectively (Fig. 2*e*; see also Fig. 7 *a* and *b*, which is published as supporting information on the PNAS web site). In contrast, SHP-2^{E76A} expressing fibroblasts increased FGF-2-mediated Ca^{2+} oscillations with a frequency of 24.2 ± 1.8 mHz (n = 8) (Figs. 2*e* and 7*c* and Movie 1). These data indicate that an activated SHP-2 mutant enhances the oscillatory frequency of Ca^{2+} in response to FGF-2. Similar gain-of-function mutants of SHP-2 cause Noonan syndrome (9, 22); therefore, we tested whether a gain-of-function mutant of SHP-2 found in Noonan syndrome (Table 2) enhances FGF-2-induced Ca^{2+} oscillatory frequency. Fibroblasts were transfected with a SHP-2 Noonan syndrome mutant in which Asp-61 is mutated to Gly-61 (SHP-2^{D61G}) (10, 11). We found that when expressed in fibroblasts, SHP-2^{D61G} also enhanced the oscillatory response evoked by FGF-2 by ≈2-fold to 21.7 ± 1.8 mHz (n = 19) (Figs. 2 *d* and *e* and 7*d*). To further characterize the oscillatory response we derived the full duration at half maxima (FDHM) for the individual Ca^{2+} peaks in the oscillatory signal. These calculations showed that the FDHM for FGF-2-triggered Ca^{2+} oscillations in vector control and SHP-2^{WT} expressing fibroblasts were 30.9 ± 3.3 s (n = 48) and 30.2 ± 2.6 s (n = 30), respectively (Fig. 2*f*). The analysis of oscillations in SHP-2^{E76A} and SHP-2^{D61G} expressing fibroblasts decreased FDHM to 15.2 ± 1.4 s (n = 36) and 22.5 ± 1.2 s (n = 53), respectively (Fig. 2*f*). Collectively, these results demonstrate that SHP-2 gain-of-function mutations as well as those found in Noonan syndrome result in enhanced Ca^{2+} oscillatory frequency and reduced FDHM.

Gain-of-Function SHP-2 Mutant Enhances Cardiomyocyte Ca^{2+} Oscillations. Increases in cytosolic Ca^{2+} through receptors such as ion channels activate calcineurin, which dephosphorylates NFAT in the

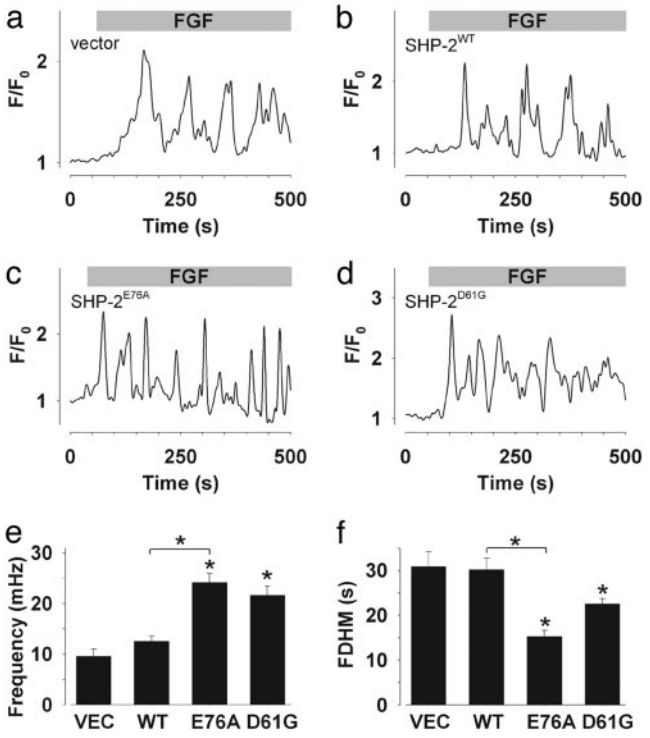

Fig. 2. Effects of gain-of-function SHP-2 mutants on Ca^{2+} signaling. (*a–d*) Intracellular Ca^{2+} recordings of FGF-2-exposed SHP-$2^{+/+}$ fibroblasts expressing vector (*a*), SHP-2^{WT} (*b*), SHP-2^{E76A} (*c*), or SHP-2^{D61G} (*d*). (*e* and *f*) Bar diagram of Ca^{2+} oscillatory frequencies (*e*) and FDHM (*f*) induced by FGF-2 derived from spectrum analysis in SHP-$2^{+/+}$ fibroblasts expressing vector (VEC), SHP-2^{WT} (WT), SHP-2^{E76A} (E76A), or SHP-2^{D61G} (D61G). Values are mean ± SEM. *, $P <$ 0.05.

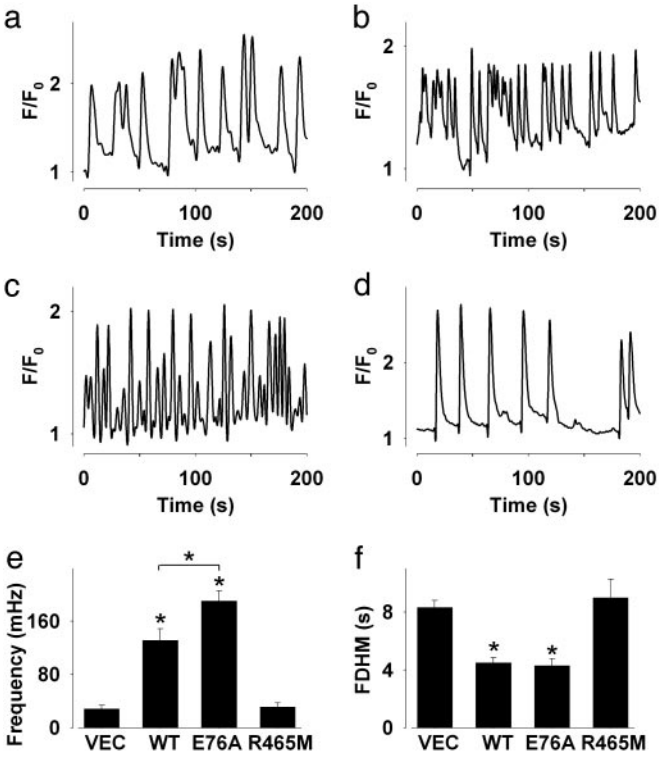

Fig. 3. SHP-2 gain-of-function mutant enhances spontaneous Ca^{2+} oscillations in cardiomyocytes. (*a–d*) Single cell traces of spontaneous Ca^{2+} oscillations in Fluo-4/AM-loaded cardiomyocytes that expresses vector (*a*), SHP-2^{WT} (*b*), SHP-2^{E76A} (*c*), or SHP-2^{R465M} (*d*). (*e* and *f*) Bar diagram of spontaneous Ca^{2+} oscillatory frequencies (*e*) and FDHM (*f*) derived from spectrum analysis in cardiomyocytes expressing vector (VEC), SHP-2^{WT} (WT), SHP-2^{E76A} (E76A), or SHP-2^{R465M} (R465M). Values are mean ± SEM. *, $P < 0.05$.

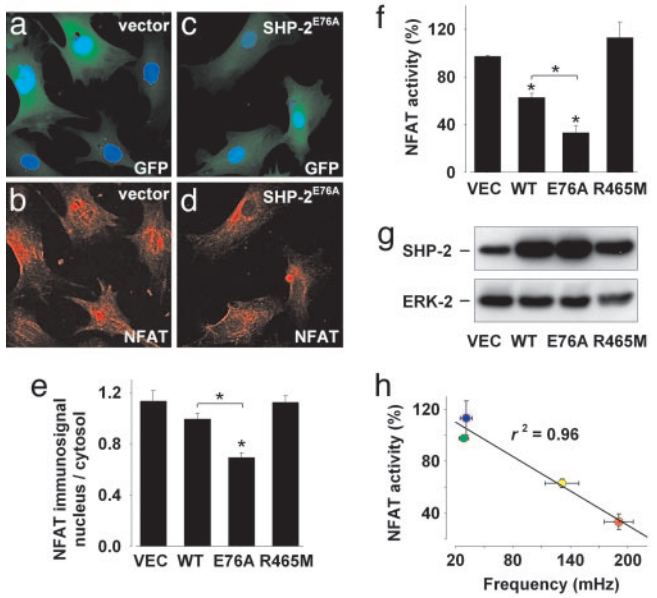

Fig. 4. Suppression of NFAT activity by SHP-2 gain-of-function mutant in cardiomyocytes. (*a–d*) Confocal images of immunostained cardiomyocytes infected with vector expressing GFP alone (green) (*a* and *b*) or GFP along with SHP-2^{E76A} (*c* and *d*). Nuclear staining with TO-PRO-3 (blue) (*a* and *c*) and NFAT expression (red) (*b* and *d*) is shown. (*e* and *f*) Statistical analysis of NFAT immunostaining (nucleus/cytosol) (*e*) and NFAT-luciferase reporter gene in cardiomyocytes (*f*) infected with vector (VEC), SHP-2^{WT} (WT), SHP-2^{E76A} (E76A), and SHP-2^{R465M} (R465M). (*g*) Immunoblot of SHP-2 expression from cell lysates used in *f* and loading controls [extracellular-regulated kinase 2 (Erk-2)]. (*h*) Bidirectional plot of NFAT activity vs. spontaneous Ca^{2+} oscillatory frequency in cells expressing vector (green circle), SHP-2^{R465M} (blue circle), SHP-2^{WT} (yellow circle), and SHP-2^{E76A} (red circle). Linear regression analysis (black line) with a correlation coefficient $r^2 = 0.96$. Values are mean ± SEM. *, $P < 0.05$.

cytosol, resulting in its translocation to the nucleus (16). Cardiac morphogenesis relies on Ca^{2+} and subsequently the precise regulation of the calcineurin/NFAT pathway (14–16). NFAT functions in numerous cellular processes, one of which involves the activation of transcription factors that regulate cardiac development (23, 24). We hypothesized that gain-of-function SHP-2 mutants would enhance Ca^{2+} oscillations in cardiomyocytes similar to those observed in fibroblasts (Fig. 2 *e* and *f*). Moreover, we speculated that altered Ca^{2+} oscillations in cardiomyocytes could interfere with calcineurin-dependent regulation of NFAT. To test this hypothesis, primary rat cardiomyocytes were first transfected with vector alone. We found that cardiomyocytes exhibited spontaneous Ca^{2+} oscillations with a frequency of 28.6 ± 5.2 mHz and FDHM of 8.3 ± 0.5 s (Figs 3 *a*, *e*, and *f* and 7*e*). Significantly, cardiomyocytes expressing SHP-2^{WT} exhibited spontaneous Ca^{2+} oscillations with a frequency of 131.2 ± 17.5 mHz and FDHM of 4.5 ± 0.3 s (Figs. 3 *b*, *e*, and *f* and 7*f*), whereas SHP-2^{E76A} cardiomyocytes responded with a spontaneous Ca^{2+} oscillation frequency of 190.5 ± 15.1 mHz and FDHM of 4.3 ± 0.5 s (Figs. 3 *c*, *e*, and *f* and 7*g*). Importantly, expression of the catalytically inactive mutant of SHP-2, SHP-2^{R465M}, was without effect as compared with vector control transfected cardiomyocytes (31.3 ± 6.4 mHz and 9.0 ± 1.3 s) (Figs. 3 *d*, *e*, and *f* and 7*h*). These data imply that constitutive SHP-2 activity gives rise to an increase in cardiomyocyte Ca^{2+} oscillatory frequency.

Suppression of NFAT Activation in Cardiomyocytes by Gain-of-Function SHP-2 Mutants. The oscillatory frequency of Ca^{2+} has been reported to be a mechanism in which calcineurin/NFAT activation can be "fine-tuned" (17–19). Moreover, NFATc1-deficient mice have defects in the formation of heart valves and the interventricular septum that resemble congenital heart defects seen in humans (23, 24). Therefore, we investigated whether enhanced SHP-2 activity affected NFAT function in cardiomyocytes. When immunostaining for NFATc1 was performed in cardiomyocytes infected with an adenovirus expressing GFP alone, an equal distribution of endogenous NFATc1 expression was observed between the nucleus and cytoplasm (Fig. 4 *a* and *b*). In contrast, cardiomyocytes infected with an adenovirus expressing SHP-2^{E76A} showed decreased nuclear expression of NFATc1 (Fig. 4 *c* and *d*). Nuclear to cytosolic expression of NFATc1 in cardiomyocytes was quantitated for vector, SHP-2^{WT}, SHP-2^{E76A} and SHP-2^{R465M} (Fig. 4*e*). This analysis showed that SHP-2^{E76A}-expressing cardiomyocytes contained ≈40% less nuclear localized NFATc1 as compared with SHP-2^{WT}-expressing cardiomyocytes (Fig. 4*e*). Moreover, the catalytically inactive mutant of SHP-2, SHP-2^{R465M}, displayed levels of nuclear NFATc1 accumulation similar to that of cardiomyocytes infected with vector and SHP-2^{WT}. These results suggest that a gain-of-function mutant of SHP-2 impairs NFATc1 nuclear localization and by inference NFAT transcriptional activity in cardiomyocytes. To confirm that NFAT transcriptional activity is functionally impaired by SHP-2^{E76A}, cardiomyocytes were coinfected with an adenoviral luciferase reporter gene driven by a NFAT minimal DNA-binding element, along with adenoviruses encoding either vector, SHP-2^{WT}, SHP-2^{E76A}, or SHP-2^{R465M}. This experiment demonstrated that SHP-2^{E76A} significantly inhibited NFAT activity by ≈30% as compared with SHP-2^{WT}-infected cardiomyocytes (Fig. 4*f*). Expression of SHP-2^{WT} was found to inhibit NFAT activity in cardiomyocytes. This result could be due to the observation that overexpressed SHP-2^{WT} also increased Ca^{2+} oscillatory frequency relative to vector control transfectants. However, the enhanced Ca^{2+} oscilla-

tory frequency seen in SHP-2^{WT} as compared with SHP-2^{E76A} was not due to differences in the expression of SHP-2 because immunoblotting of the same lysates used for the NFAT reporter gene experiments showed comparable levels of SHP-2 in SHP-2^{WT}- and SHP-2^{E76A}-expressing cardiomyocytes (Fig. 4*g*). Significantly, NFAT activity in SHP-2^{R465M}-expressing cardiomyocytes was not inhibited, although SHP-2^{R465M} was overexpressed relative to vector control-infected cardiomyocytes (Fig. 4 *f* and *g*). These results support the interpretation that enhanced SHP-2 activity suppresses NFAT activation. Finally, we performed a two-way analysis, correlating NFAT activity in response to the expression of SHP-2^{WT}, SHP-2^{E76A}, and SHP-2^{R465M} with their respective Ca^{2+} oscillatory frequencies generated in cardiomyocytes. This analysis revealed a correlation coefficient of $r^2 = 0.96$ for vector, SHP-2^{WT}, SHP-2^{E76A}, and SHP-2^{R465M} vs. their respective cardiomyocyte Ca^{2+} oscillatory frequencies (Fig. 4*h*). Thus, SHP-2 catalysis correlates with an increase in Ca^{2+} oscillatory frequency and suppression of NFAT activation in cardiomyocytes.

Discussion

Our data show that SHP-2 is responsible for evoking distinct Ca^{2+} responses after stimulation of fibroblasts with either PDGF or FGF-2. We found that PDGF produced a Ca^{2+} transient whereas FGF-2 generated Ca^{2+} oscillations, and in both of these cases Ca^{2+} responses were abrogated in fibroblasts lacking functional SHP-2. Importantly, SHP-2 does not participate in all receptor-mediated Ca^{2+} signaling pathways because loss of functional SHP-2 in fibroblasts still resulted in Ca^{2+} mobilization upon activation of the G protein-coupled P2Y receptor. These data demonstrate that SHP-2 is responsible for generating Ca^{2+} responses downstream of RTKs but not G-protein-coupled receptors. Furthermore, SHP-2 appears to mediate distinct Ca^{2+} responses among different RTKs. How SHP-2 regulates Ca^{2+} transients and oscillations, however, remains to be established. The Src-family kinases can activate phospholipase Cγ1, which mediates the release of $InsP_3$ and subsequently Ca^{2+} mobilization. The catalytic activity of SHP-2 has been shown to be responsible for the activation of the Src-family kinases (25). Thus, Src-family kinase phosphorylation of phospholipase Cγ1 mediated by SHP-2 in response to RTK activation is one candidate pathway through which SHP-2 may mediate Ca^{2+} release. Indeed, it was shown recently that SHP-2 is required for the mobilization of Ca^{2+} in response to interleukin-1 by a mechanism involving phospholipase Cγ1 tyrosine phosphorylation (26). Our data support this idea because we show specifically that the catalytic activity of SHP-2 is required for FGF-2-induced Ca^{2+} mobilization.

One of the key findings of this work is that enhanced catalytic activity of SHP-2 rendered by a gain-of-function mutation resulted in a significant increase in the Ca^{2+} oscillatory frequency and a significant FDHM decrease in response to FGF-2 in fibroblasts and primary cardiomyocytes. Gain-of-function SHP-2 mutants have been shown to cause hyperactivation of the extracellular-regulated kinases (ERKs) and to increase cell proliferation (11). Our results now show that the Ca^{2+} signaling pathway is also a target for aberrant regulation by gain-of-function SHP-2 mutants. Many mutations in SHP-2 that are associated with Noonan syndrome occur at the interface between the PTP domain and NH_2-terminal SH2 domain resulting in its constitutive activation (9). We show that in addition to the gain-of-function SHP-2^{E76A} mutant, SHP-2^{D61G} mutation, which is found in Noonan syndrome patients, also resulted in enhanced Ca^{2+} oscillatory frequency and decreased FDHM in response to FGF-2. Therefore, our results suggest that altered Ca^{2+} signaling, conferred by SHP-2 gain-of-function mutants found in Noonan syndrome, may be a related molecular mechanism associated with the pathogenesis of this disease. Interestingly, patients with Leopard syndrome, a closely related developmental disorder to that of Noonan syndrome in which SHP-2 mutations have been identified, suffer from electrocardiographic conduction abnormalities (10). Our observation that gain-of-function SHP-2 mutants disrupt the "pacemaker" feature of cardiomyocytes provides insight into potential mechanisms for why Leopard syndrome patients manifest with electrocardiographic conduction defects.

Noonan syndrome patients often present with cardiovascular abnormalities, primarily congenital heart diseases in up to 85% of affected individuals. The most prevalent form of congenital heart disease in Noonan syndrome is pulmonic stenosis, in addition to other lesions such as atrioventricular septal defects, mitral valve abnormalities, and hypertrophic cardiomyopathy (7, 8). A number of signaling pathways have been implicated in cardiac morphogenesis. Notably, the NFAT signaling pathway has been shown to be critical for cardiac development and is regulated by Ca^{2+} through the actions of calcineurin (13–16). We tested the hypothesis that altered Ca^{2+} signaling evoked by SHP-2 gain-of-function mutations might disrupt NFAT function. Our data demonstrate that enhanced Ca^{2+} oscillatory frequency induced by SHP-2 gain-of-function mutants in cardiomyocytes correlates with the inhibition of NFAT translocation to the nucleus and subsequently suppression of NFAT transcriptional activity. These data implicate NFAT as a target of SHP-2 gain-of-function/Noonan syndrome mutants. Provocatively, altered NFAT function in mice through genetic ablation gives rise to valvulogenesis defects (23, 24) that bear some similarity to the congenital heart defects observed in a mouse model of Noonan syndrome (12). There is good evidence that calcineurin which activates NFAT by dephosphorylation is regulated not just by increases in intracellular Ca^{2+} but also by the oscillatory frequency of Ca^{2+} (27). After NFAT translocation to the nucleus, it also has been shown that NFAT transcriptional activity is modulated by the frequency of intracellular Ca^{2+} oscillations (17, 18). The fact that SHP-2 gain-of-function mutations decreased the FDHM also might contribute to the NFAT transcriptional activity. Thus, it is conceivable that altered Ca^{2+} signaling and/or disruption of the NFAT function by Noonan syndrome mutants may contribute to the development of congenital heart abnormalities.

In summary, we show that the catalytic activity of SHP-2 is required for FGF-2-induced Ca^{2+} oscillations in fibroblasts. Moreover, constitutive SHP-2 catalysis, as exhibited in gain-of-function/Noonan syndrome SHP-2 mutations, resulted in enhanced Ca^{2+} oscillatory frequency in response to FGF-2 in fibroblasts and spontaneous Ca^{2+} oscillations in cardiomyocytes. Both the FGF and the Ca^{2+}/calcineurin/NFAT pathways are critical for cardiac morphogenesis (14, 28). SHP-2 gain-of-function mutants perturb the Ca^{2+} oscillatory frequency downstream of the FGF receptor, which could contribute to abnormal cardiac morphogenesis. Perturbations in NFAT function through dysregulation of the Ca^{2+}/calcineurin/NFAT axis in cardiomyocytes also appears to be a pathway through which gain-of-function/Noonan syndrome mutants of SHP-2 may disrupt cardiac valvulogenesis (14). Collectively, these results provide a potential mechanistic link between SHP-2 gain-of-function mutants and the development of congenital heart disease seen in Noonan syndrome.

Materials and Methods

Cell Cultures. Fibroblasts derived from mice containing either a deletion within exon 3 of SHP-2 that removes amino acids 46–110 of the NH_2 terminus SH2 domain (SHP-$2^{Ex3-/-}$) or from WT (SHP-$2^{+/+}$) littermate controls are described in refs. 4 and 29. Briefly, cells were cultured at 37°C and 5% CO_2 in DMEM (Invitrogen) containing 10% FBS (Sigma), 1 mM sodium pyruvate (Invitrogen), 5 units/ml penicillin, and 50 μg/ml streptomycin (Sigma). Cardiac myocytes were prepared as described in ref. 30. Primary cultures of cardiomyocytes were cultured from hearts of 1- to 3-day-old Sprague–Dawley rats seeded on gelatin-coated coverslips and starved in serum-free medium 24 h prior to the experiment. The protocol produces cultures of cardiac myocytes that are at least 95% pure (30).

Plasmids and Adenoviruses. pIRES-DsRed plasmids containing either SHP-2^{WT} or gain-of-function/Noonan syndrome mutants of SHP-2 (SHP-2^{E76A} and SHP-2^{D61G}) or a catalytically inactive mutant of SHP-2 (SHP-2^{R465M}) were prepared as described in ref. 31. Transient transfections were performed by using Lipofectamine 2000 (Invitrogen) in OptiMEM. After transient transfections, cells were serum-starved for 16–24 h before the experiments in DMEM containing 0.1% FBS. Purified FGF-2–GFP protein was provided by Joseph Schlessinger (Yale University School of Medicine, New Haven, CT). Adenoviruses encoding for the expression of SHP-2^{WT} and SHP-2^{E76A} were generated as described in ref. 31.

Calcium Measurements. Cells were incubated (30 min at 37°C in 5% CO_2) in Hepes medium containing 5 μM Fluo-4/AM (Molecular Probes) together with 0.1% Pluronic F-127 (Molecular Probes). The Hepes medium contained 130 mM NaCl, 4.7 mM KCl, 1.3 mM $CaCl_2$, 1 mM $MgSO_4$, 1.2 mM KH_2PO_4, 20 mM Hepes (pH 7.4), and 5 mM dextrose. Coverslips were mounted in a temperature-controlled (37°C) chamber (Warner Instruments, Hamden, CT) and transferred to a Zeiss LSM 510 META scanning laser confocal microscope equipped with a C-Apochromat ×40/1.2 water immersion objective (Zeiss). Images were acquired at 0.2 Hz for the fibroblast cells and 0.5 Hz for the cardiac myocytes. All drugs were bath applied.

Immunocytochemistry. Immunocytochemical staining of NFAT and $InsP_3Rs$ was performed according to standard protocol, using fixation by 4% paraformaldehyde in 1 h. After blocking with 1% BSA, cells were incubated with NFATc1 C20 goat polyclonal antibody (Ab) (1:100, Santa Cruz Biotechnology) for 1 h and then with Alexa 546 fluorescent secondary Ab (1:200; Molecular Probes) for 1 h, together with 0.3% Triton X-100. Nucleus was stained with TO-PRO-3 (1:200; Molecular Probes) for 10 min. $InsP_3Rs$ were stained by using the same protocol with the following Abs: polyclonal type-1 $InsP_3R$ Ab (1:20,000; custom-produced by Research Genetics, Huntsville, AL), polyclonal type-2 $InsP_3R$ Ab (1:250; generously provided by F. Leite, Federal University of Minas Gerais, Belo Horizonte, Brazil), and mouse monoclonal type-3 $InsP_3R$ Ab (1:500; BD Biosciences), and then with Alexa 488 fluorescent secondary Ab (1:500; Molecular Probes) for 1 h. Slides were scanned by using a Zeiss LSM510 META confocal scanning laser microscope equipped with a C-Apochromat 40×/1.2 water immersion objective (Zeiss).

Immunoblot Analyses. Cell lysates were prepared and immunoblotting was performed as described in ref. 31. Abs used were as follows: polyclonal SHP-2 Ab (Santa Cruz Biotechnology), polyclonal type-1 $InsP_3R$ Ab (custom-produced by Research Genetics), polyclonal type-2 $InsP_3R$ Ab (generously provided by F. Leite), and monoclonal type-3 $InsP_3R$ Ab (BD Biosciences).

Adenoviral NFAT–Luciferase Infection and Luciferase Reporter Assay. The adenoviral NFAT–luciferase reporter (AdNFAT-luc) construct was generously provided by Jeffery D. Molketin (Children's Hospital Medical Center, Cincinnati) and is described in ref. 32. Cardiomyocytes were infected with pAd-GFP, Ad-WT, Ad-E76A, or Ad-R465M and Ad-NFAT-Luc for 2 h before switching to fresh growth medium. Cultures were incubated for 48 h before harvesting. Lysates were generated and luciferase activity was determined according to the manufacturer's instructions by using the Luciferase Assay System (Promega). Luciferase activity was normalized to total protein concentration for each sample as determined by Coomassie Protein Assay Reagent (Pierce), and results were expressed as relative luciferase units per microgram of protein (RLU/μg).

Chemicals. Chemicals used were as follows: ATP, bradykinin, CPA, thapsigargin, 2-aminoethoxydiphenyl borate (2-APB) (all from Sigma), FGF-2, and PDGF (Calbiochem). All drugs were bath applied.

Data Analysis. Power spectrum analysis was carried out as described in ref. 21. Briefly, a power spectrum of a signal is the squared magnitude of its Fourier transform and describes the contribution to a signal by each of its sine wave components. In the power spectrum, each peak corresponds to a different frequency present in the original data. The peak with highest power spectral density (PSD) indicates the most dominant frequency within the Ca^{2+} signal. Oscillations were analyzed in a program written in MATLAB (21). The frequency resolution was 3.1 mHz. The time duration for individual peaks in the Ca^{2+} oscillatory response was analyzed by calculating the FDHM using an algorithm implemented in MATLAB. Briefly, the FDHM value for a Ca^{2+} peak is given by the time difference between the two points on each side of the peak at which the Ca^{2+} level reaches half its maximum value. Data are presented as means ± SEM of a minimum of three experiments, unless indicated otherwise. Student's t test was used, and significance was accepted at $P < 0.05$. Regression analysis and correlation coefficient r^2 were computed by using SIGMAPLOT (Systat, Evanston, IL).

This work was supported by National Institutes of Health Grants P01 DK57751 (to A.M.B. and B.E.E.) and AR46504 (to A.M.B.), a grant from the Muscular Dystrophy Association (to A.M.B.), and a grant from Vetenskapsrådet–the Swedish Research Council to (to P.U.).

1. Neel, B. G., Gu, H. & Pao, L. (2003) *Trends Biochem. Sci.* **28,** 284–293.
2. Hof, P., Pluskey, S., Dhe-Pagganon, S., Eck, M. J. & Shoelson, S. E. (1998) *Cell* **92,** 441–450.
3. O' Reilly, A., Pluskey, S., Shoelson, S. E. & Neel, B. G. (2000) *Mol. Cell. Biol.* **20,** 299–311.
4. Saxton, T. M., Henkemeyer, M., Gasca, S., Shen, R., Rossi, D. J., Shalaby, F., Feng, G. S. & Pawson, T. (1997) *EMBO J.* **16,** 2352–2364.
5. Chen, B., Bronson, R. T., Klaman, L. D., Hampton, T. G., Wang, J. F., Green, P. J., Magnuson, T., Douglas, P. S., Morgan, J. P. & Neel, B. G. (2000) *Nat. Genet.* **24,** 296–299.
6. Saxton, T. M., Ciruna, B. G., Holmyard, D., Kulkarni, S., Harpal, K., Rossant, J. & Pawson, T. (2000) *Nat. Genet.* **24,** 420–423.
7. Noonan, J. A. (1994) *Clin. Pediatr.* **33,** 548–555.
8. Noonan, J. A. (1968) *Am. J. Dis. Child* **116,** 373–380.
9. Tartaglia, M., Mehler, E. L., Goldberg, R., Zampino, G., Brunner, H. G., Kremer, H., van der Burgt, I., Crosby, A. H., Ion, A., Jeffery, S., *et al.* (2001) *Nat. Genet.* **29,** 465–468.
10. Tartaglia, M. & Gelb, B. D. (2005) *Eur. J. Med. Genet.* **48,** 81–96.
11. Tartaglia, M., Niemeyer, C. M., Fragale, A., Song, X., Buechner, J., Jung, A., Hahlen, K., Hasle, H., Licht, J. D. & Gelb, B. D. (2003) *Nat. Genet.* **34,** 148–150.
12. Araki, T., Mohi, M. G., Ismat, F. A., Bronson, R. T., Williams, I. R., Kutok, J. L., Yang, W., Pao, L. I., Gilliland, D. G., Epstein, J. A. & Neel, B. G. (2004) *Nat. Med.* **10,** 849–857.
13. Runyan, R. B., Potts, J. D., Sharma, R. V., Loeber, C. P., Chiang, J. J. & Bhalla, R. C. (1990) *Cell Regul.* **1,** 301–313.
14. Chang, C. P., Neilson, J. R., Bayle, J. H., Gestwicki, J. E., Kuo, A., Stankunas, K., Graef, I. A. & Crabtree, G. R. (2004) *Cell* **118,** 649–663.
15. Wilkins, B. J. & Molkentin, J. D. (2004) *Biochem. Biophys. Res. Commun.* **322,** 1178–1191.
16. Crabtree, G. R. & Olson, E. N. (2002) *Cell* **109,** Suppl., S67–S79.
17. Dolmetsch, R. E., Lewis, R. S., Goodnow, C. C. & Healy, J. I. (1997) *Nature* **386,** 855–858.
18. Dolmetsch, R. E., Xu, K. & Lewis, R. S. (1998) *Nature* **392,** 933–936.
19. Li, W., Llopis, J., Whitney, M., Zlokarnik, G. & Tsien, R. Y. (1998) *Nature* **392,** 936–941.
20. Berridge, M. J., Bootman, M. D. & Roderick, H. L. (2003) *Nat. Rev. Mol. Cell. Biol.* **4,** 517–529.
21. Uhlen, P. (2004) *Sci. STKE* **2004,** pl15.
22. Tartaglia, M., Kalidas, K., Shaw, A., Song, X., Musat, D. L., van der Burgt, I., Brunner, H. G., Bertola, D. R., Crosby, A., Ion, A., *et al.* (2002) *Am. J. Hum. Genet.* **70,** 1555–1563.
23. Ranger, A. M., Grusby, M. J., Hodge, M. R., Gravallese, E. M., de la Brousse, F. C., Hoey, T., Mickanin, C., Baldwin, H. S. & Glimcher, L. H. (1998) *Nature* **392,** 186–190.
24. de la Pompa, J. L., Timmerman, L. A., Takimoto, H., Yoshida, H., Elia, A. J., Samper, E., Potter, J., Wakeham, A., Marengere, L., Langille, B. L., *et al.* (1998) *Nature* **392,** 182–186.
25. Zhang, S. Q., Yang, W., Kontaridis, M. I., Bivona, T. G., Wen, G., Araki, T., Luo, J., Thompson, J. A., Schraven, B. L., Philips, M. R. & Neel, B. G. (2004) *Mol. Cell* **13,** 341–355.
26. Wang, Q., Downey, G. P., Herrera-Abreu, M. T., Kapus, A. & McCulloch, C. A. (2005) *J. Biol. Chem.* **280,** 8397–8406.
27. Tomida, T., Hirose, K., Takizawa, A., Shibasaki, F. & Iino, M. (2003) *EMBO J.* **22,** 3825–3832.
28. Lavine, K. J., Yu, K., White, A. C., Zhang, X., Smith, C., Partanen, J. & Ornitz, D. M. (2005) *Dev. Cell* **8,** 85–95.
29. Zito, C. I., Kontaridis, M. I., Fornaro, M., Feng, G. S. & Bennett, A. M. (2004) *J. Cell. Physiol.* **199,** 227–236.
30. Ibarra, C., Estrada, M., Carrasco, L., Chiong, M., Liberona, J. L., Cardenas, C., Diaz-Araya, G., Jaimovich, E. & Lavandero, S. (2004) *J. Biol. Chem.* **279,** 7554–7565.
31. Kontaridis, M. I., Eminaga, S., Fornaro, M., Zito, C. I., Sordella, R., Settleman, J. & Bennett, A. M. (2004) *Mol. Cell. Biol.* **24,** 5340–5352.
32. Wilkins, B. J., Dai, Y. S., Bueno, O. F., Parsons, S. A., Xu, J., Plank, D. M., Jones, F., Kimball, T. R. & Molkentin, J. D. (2004) *Circ. Res.* **94,** 110–118.